1 Heading text

This is a ^{sentence} ***that*** contains text ***with*** ~~different~~ $_{formatting}$.

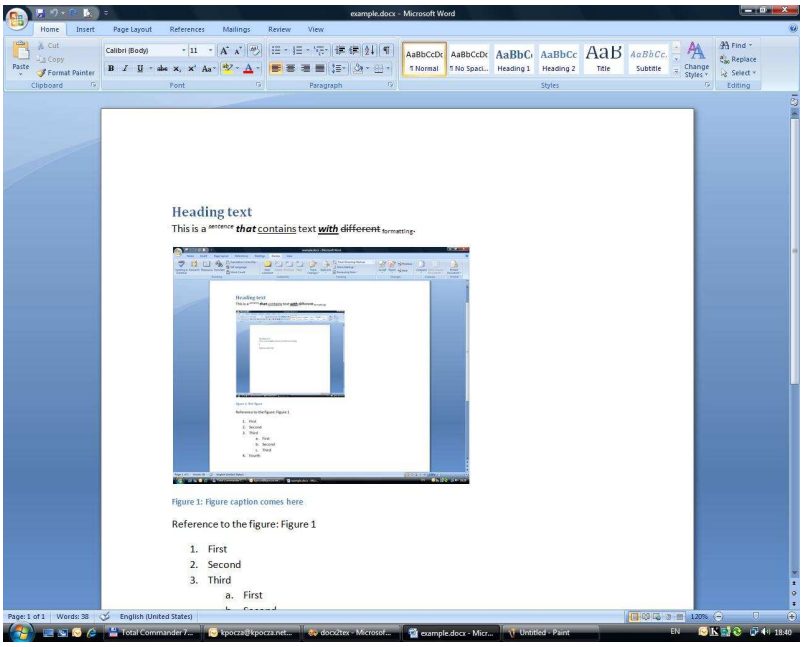

Figure 1: : Figure caption

Reference to the figure: 1.

1. First
2. Second
3. Third
   (a) First
   (b) Second
   (c) Third
4. Fourth

1	2
3	4

Table 1: : caption

Table Caption: 1.

1.1 This is a second heading

árvíztűrő tükörfúrógép

ÁRVíZTŰRŐ TÜKÖRFÚRÓGÉP

Underlined

italic

fat

underlineditalic

italicfat

underlinedfat

underlineditalicfat

1. egy
2. kettő
3. három
   (a) a
   (b) b
   (c) c
4. négy

---

5. aaa
6. bbb
7. ccc

1.1.1 This is a third heading

- a
- b
  - b1
    - b1A
    - b2A
  - b2
  - b3

- c
- d

1. AAA
2. BBB
3. CCC

<> as'q . . . # \ { } % ˜ _ ˆ & $ ” ”
EFG
HIJK
~~A~~ $\not{b}\not{/}^{cdef}_{defin}$

Ez egy hosszú paragraph, amelyet balra igazítottunk. Még írok ide cuccot, hogy látszódjon a dolog, legalább is word-ben.

Ez egy hosszú paragraph, amelyet jobbra igazítottunk. Még írok ide, hogy látszódjon a dolog, legalább is word-ben.

Ez egy hosszú paragraph, amelyet centerre igazítottunk. Még írok ide, hogy látszódjon a dolog, legalább is word-ben.

Ez egy hosszú paragraph, amelyet justify igazítottunk. Még írok ide, hogy látszódjon a dolog, legalább is word-ben. Írok még egy sort, hogy teljesen korrektül látszódjon a formázás. Nézzük meg, hogy mi történik latex-ben.

Section: 1.
SubSection: 1.1.
SubSubSection:1.1.1.
Math formulas:
$B(a) = x + \sqrt[3]{a}$

$\sum_a^b c \prod_{n=1..k} n$

The adaptive fit of a phenotype to its environment follows from the degree to which selection and mutation act on that phenotype. We may view vital rates (i.e., age-specific survival and reproduction) as adaptations, each of which is a complex phenotype determined by numerous genetic and environmental factors. Because the strength of selection declines with age (HAMILTON 1966), we expect differential adaptation leading towards relatively lower rates of early-age mortality and, all else being equal, greater rates of reproduction at younger ages. This perspective views senescence as

a manifestation of an age-related loss in adaptation. If mutational effects are themselves dependent upon the degree of adaptation, as suggested by FISHER (1958), then the effects of mutations will depend upon the age at which they act. Mutations will tend to be most deleterious when purifying selection against the mutational load is at its greatest. This positive association between the influx of deleterious mutational load (greatest at early age) and purifying selection (also greatest at early age) will tend to dampen the age-related changes in vital rates at mutation-selection equilibrium. In other words, negative feedback between mutation and selection will cause less senescence than is predicted by the standard mutation accumulation model of aging. We explore this consequence of Fisher's model on the evolution of age-specific mortality using numerical simulations.

Adaptive Geometry: FISHER (1958) argued that because fitness is the result of great physiological and environmental complexity, the trajectory of trait adaptation towards an optimum will be constrained to a serial process of small improvements. To illustrate this point, he introduced a heuristic " geometric model of adaptation". This model imagines a phenotype represented by a point P that is separated from an optimum O in n -dimensional phenospace by some Euclidian distance z (Figure 1), where n is the number of traits that affect the phenotype and are under selection. This phenospace represents the entire universe of possible multivariate phenotypic configurations. As all points at some distance from the optimum are equivalent, the phenotype can be imagined as a circle, sphere, or, more generally, a hypersphere with a characteristic radius equal to z. A change in the phenotype, such as might follow from a mutation, will move the genotype away from P by some amount r. Fisher noted that the probability that such a change moves the phenotype closer to the optimum (thereby increasing fitness) decreases with increasing r and n. Specifically, the probability that a mutation is beneficial is approximated by the cumulative standard normal distribution,

$$B(v) \cong \frac{1}{\sqrt{2\pi}} \int_v^\infty e^{-\frac{t^2}{2}} dt \quad (1),$$

where $= \frac{r\sqrt{n}}{z}$, the effective size of the mutation, and n, the dimensionality of the trait, is very large (FISHER 1958; KIMURA 1983; LEIGH 1987; ORR 1998; RICE 1990). Fisher's model offers a useful heuristic means with which to think about the distribution of mutational effects.

Age-structure complicates adaptive geometry: Here, we extend Fisher's model to explore how the distribution of mutational effects might change with age and with the complexity of vital rates. The fit of a phenotype to a particular environment determines the radius of the adaptive geometry. Because the selection that drives adaptation is attenuated with age, more deleterious age-specific mutations are allowed to accumulate at

late age (HAMILTON 1966). We expect that the age-specific radii of phenotypes P will consequently increase with age, becoming less well adapted to their age-specific environments. We extend Fisher's heuristic model by adding a temporal dimension x. The result is a series of hyperspheres, each representing the n_x-dimensional adaptive geometry specific to a particular age class. Each age-specific hypersphere has some radius, z_x, which follows from the degree of adaptation characteristic of the age-specific phenotypes. All else being equal, these radii increase with age after the age of reproductive maturity is reached because the intensity of selection lessens with age. Because selection for survival is not expected to change prior to reproductive maturity, all pre-reproductive hyperspheres will have the same radii provided that the influx of mutational effects does not change (this assumes that n_x is constant - see below).

Previous applications of Fisher's model illustrate the adaptive geometry of a population using the simplest two-dimensional projection of the hypersphere, the circle (e.g., HARTL and TAUBES 1996; ORR 1998; ORR 2006; POON and OTTO 2000; WAXMAN 2006). In keeping with this tradition, we imagine a series of circles with radii that increase with age. We standardize the age-specific radius for dimensionality by dividing each radius z_x by the square root of n_x (Equation 1). When we align the age-ranked circles that represent the radii of reproductive ages along the temporal axis that runs perpendicular to the age-specific radii, we form a truncated cone (a conical frustum). As the intensity of selection on mortality is expected to be constant for all pre-reproductive ages (HAMILTON 1966) and provided that complexity is constant, the circles for these earliest age-classes will form a column with a radius that is equal to the smallest radius of the frustum (Figure 2). We define the adaptive geometry of the whole life course by appending the pre-reproductive cylinder to the frustum formed by the reproductively mature age-classes. Taken together, the age-specific shape of the adaptive geometry appears as a funnel in a three-dimensional projection. The adaptive geometry of a phenotype at a particular age is recovered by taking a cross-section of the funnel perpendicular to the temporal axis.

Geometric interpretations of age-specific mutational effects: At a single age, a mutational effect on this phenospatial scale can be defined by an n_x-dimensional vector with Euclidean length r. However, the effect of a mutation over all ages is far more complex because a single mutation can have an effect on the phenospace at any or all ages. This effect can vary freely in magnitude and direction, although the tendency to do so depends upon the degree to which an organism's physiology and environment are integrated across ages. In light of the model shown in Figure 2, we can visualize a mutation with identical phenospatial effects at all ages as a line running

parallel to the funnel surface. Aside from its effects on this multidimensional phenospatial scale, a mutation may also have an effect on the univariate fitness scale. This is a change in the spatial distance z between the optimum and the new phenotype's adaptive position P. A mutation is consistently beneficial (or deleterious) if it is always within (or always outside) the surface of the volume. These types of mutations will contribute to positive fitness correlations across ages. Mutational effects that enter and exit the volume at different places along x will contribute to negative fitness correlations across ages - a requirement for antagonistically pleiotropic mechanisms for the evolution of senescence.

In the *window-effect* model (CHARLESWORTH 2001), the effects of a mutation are neutral until some age$x$, have some constant effect over Δx, and then return to neutrality. We can visualize the effect of this form of mutational effect by imagining a line traveling along the surface of the funnel (Figure 3). At some point that corresponds to the earliest age defining the window, the line juts outwards (a deleterious mutational effect) or inwards (a beneficial mutational effect) in a direction perpendicular to the temporal axis. After traveling some distance corresponding to the magnitude of the effect (the greater the distance, the greater the effect), the line then resumes a course parallel to the surface of the funnel. Upon reaching the end of the window (i.e., the age of last effect), the line returns to the surface of the funnel and continues to run uninterrupted along the surface of the funnel to its terminus. With continuous-time models, the window of time becomes infinitesimally small (i.e., $\Delta x \rightarrow 0$) and the number of age classes becomes infinitely large. We can attribute the frequent use of the window model in theoretical explorations of aging to its apparent simplicity: the duration of the effects of mutations is constrained to the size of the window, which can define a single age-class. There can be no genetic correlations across ages either among mutations or among the genetic variants that segregate at mutation-selection equilibrium. As a result, it is straightforward to predict evolutionary trajectories. We consider this model in our simulations.

Numerical simulations of age-specific mortality: We wished to understand how these adaptation-dependent mutational effects influence the evolution of senescence as reflected by declines in survival rates with age. Because we are particularly interested in the effect of mutations on age-specific mortality, we set the within-age class variance in reproductive output to zero, thereby assuming that the variation in age-specific fitness depends entirely upon three factors-the variation in age-specific survival, reproduction as a function of age, and the age-structure of the population. This allowed us to equate the concept of adaptive geometry to a geometry of age-specific survival. We viewed survival at each age (or its negative natural logarithm,

mortality) as independent phenotypes made up of many (n_x) traits under selection. The simultaneous effects of window-effect mutations (i.e., a given mutation affects one and only one of the non-overlapping windows) and selection upon the mean and variance of age-specific survival at mutation-selection equilibrium were explored using deterministic simulation models of an age-structured infinite-size population coded in R 2.5.1 (R DEVELOPMENT CORE TEAM 2007). Our goal was to explore 1) how the mean and variance of mortality (defined as the negative logarithm of survival rates) evolve and 2) how the mean and variance of mutational effects on mortality change with age when the effects of age-specific mutations depend upon the adaptive fit of individuals at each age.

We imagined an infinite population that experienced cycles of reproduction, mutation, and viability selection for some time T sufficient to reach demographic and genetic equilibria. The demographic structure of a population with X age classes at time t was described by the probability density function $\pi_{y,t}$, where y is the age of the cohort. There were $X-1$ survival traits; each determined the probability that an individual successfully transitioned from age x to age $x+1$. Mutations acted on single age classes, corresponding to a window effect model of mutation with $\Delta x = 1$. Each individual that successfully transitioned from age x to age $x+1$ contributed offspring to the offspring pool with age-specific fecundity m_x. The probability at time t that an individual belonging to y has an age x-specific phenotype (the distance to the age-specific optimum) equal to z is $p_{z,x,y,t}$. Cohorts expressed these phenotypes when $y = x$. Otherwise the phenotypes were latent, having been expressed before (if $y > x$) or waiting to be expressed in the future ($y < x$). We defined survival as an exponential function of phenospatial distances, $P_z = e^{-z}$, because survivorship mutations are usually considered to act additively on the log scale (CHARLESWORTH 1994; HAMILTON 1966 - but see BAUDISCH 2005). Thus, the distance of a phenotype from the optimum defined its age-specific mortality exactly, $z = \mu_x = -\ln(P_z)$.

We explored the case of four age classes ($X = 4$) with three transition traits determining the survival probabilities. The distance z (mortality) ranged from 0.0025 to 10.0025 and was binned into classes of size 0.005. Thus, there were 2000 possible phenotypes available to each individual at each age x. At any time t there were nine phenotypic distributions (three cohorts each with three age-specific phenotypes), we represented each of these with a vertical vector $p_{x,y,t}$. This is the distribution of distance z for age x among cohort y at time t. Initially, the population's age distribution and age-specific breeding value distributions were uniform: $\pi_{x,1} = \frac{1}{X}$and $p_{z,x,y,1} = \frac{1}{2000}$ for all x, y, and z. Differently put, age-specific survival within ages was highly variable but there was no mean change in survival with age (i.e., no initial

senescence).

A long held conclusion of life history theory is that age-related increases in fecundity will mitigate (but not completely eliminate) the evolution of senescence by increasing the relative intensity of selection on late-age survival (WILLIAMS 1957). To explore the effect of varying late-age selection on survival, we considered three different reproductive functions, $m_1 = \{0, 1, 1\}$, $m_2 = \{0, 1, 2\}$,and $m_3 = \{0, 1, 4\}$ with the expectation that age-specific selection will decline with age most with m_1 and least with m_3. In each treatment, reproduction was delayed until after the second transition. This provided one test of our simulation model: because the decline in selection associated with age was deferred until the onset of reproduction, we expected no change in equilibrium mortality associated with the first two transitions when the mortality effects of mutations were held constant. Any differences in mortality rates at mutation-selection equilibrium between the first two transitions could not be due to differences in selection. We designate the three age-specific survival traits as: juvenile survival (transitioning from $x = 1to2$), early adult survival (from $x = 2to3$), and late adult survival (from $x = 3to4$).

Viability selection: Every cohort had $X - 1$ phenotypic distributions, each corresponding to mortality at a different age. At each time step, selection changed the phenotypic distributions in each cohort that corresponded to mortality at that time, $x = y$. Following our definition of bins and the survival function, age-specific survival could range from a high of 99.75% to a low of less than 0.00005%. We defined a vertical vector s in which each element corresponds to the survival of a phenotype, $s = e^{-z}$, where $z = \{\frac{1}{400}, \frac{3}{400}, \cdots, \frac{4001}{400}\}$. The distributions of phenotypes currently under selection are described by $p_{y,y,t}$. After selection, these distributions were re-weighted by their phenotype-specific viability,

$$p_{y,y+1,t+1} = \frac{s \cdot p_{y,y,t}}{s^T \cdot p_{y,y,t}} \quad (2).$$

Other distributions $x \neq y$ were shielded from selection. Thus

$$p_{x,y+1,t+1} = p_{x,y,t} \quad (3).$$

We standardized the age-distributions to correct for mortality and the production of new offspring. First, we found the un-standardized size of each cohort at time $t + 1$ that followed from viability selection,

$$\pi'_{y+1,t+1} = \pi_{y,t} \times s^T \cdot p_{y,y,t} \quad (4).$$

The size of each new cohort $y = 1$ follows from the previous age-structure $\pi_{y,t}$ and the age-specific fecundity function m, $\pi'_{1,t+1} = \sum_{y=1}^{Y} \pi_{y,t} \cdot m_y$. We standardize the new age-structure to account for this new cohort,

$$\pi_{y,t+1} = \frac{\pi'_{y,t+1}}{\sum_{y=1}^{Y} \pi_{y,t+1}} \quad (5).$$

Reproduction and mutation: All surviving individuals reproduced asexually at the end of each time period t. Phenotypes were assumed to

be completely heritable, excepting the effects of mutation (like POON and OTTO (2000),we ignore environmental variation). To model the distribution of mutation effects, we followed closely the mutation model of POON and OTTO (2000). The effect of mutation on all phenotypic traits was assumed to be distributed as a set of n independent reflected exponentials (symmetric about zero) each with the same parameter λ. Under this assumption, the magnitude r was distributed as

$$p(r,n) = \frac{\lambda^n e^{-\lambda r} r^{n-1}}{\Gamma(n)} \quad (6),$$

and the angle θ as

$$p(\theta,n) = c^{'} \sin^{n-2}\theta, \quad (7),$$

where

$$c^{'} = \frac{\Gamma(\frac{n}{2})}{\sqrt{\pi}\Gamma[\frac{1}{2}(n-1)]} \quad (7a).$$

For some initial distance z, mutational distance r , and effective orientation *?*, the distance of the changed phenotype from the optimum was

$$z^{'} = \sqrt{z^2 + r^2 - 2zrcos\theta} \quad (8).$$

We re-arranged Equation 8 to find the angle of mutational effect that caused the distance to transition from distance z to $z^{'}$,

$$\theta(z,r,z^{'}) = \cos^{-1}(\frac{z^2+r^2-z^{'2}}{2zr}) \quad (9).$$

We used Equations 6-9 to find the probability that a mutation at distance z would end up within some distance $\pm\frac{1}{400}$ from every possible value of z. The probability that a mutation shifts the phenotype from z to the interval $z^{'} \pm \frac{1}{400}$ was

$$Pr\{z+\Delta z-\tfrac{1}{400} < z^{'} < z+\Delta z+\tfrac{1}{400}\} = \int_{r=\Delta z}^{Z+z} \int_{\theta(z,r,z+\Delta z-\frac{1}{400})}^{\theta(z,r,z+\Delta z+\frac{1}{400})} p(r,n)p(\theta,n)d\theta dr$$

(10).

Mutations with effect $r > Z + z$ caused the new phenotype to equal Z, making Z an absorbing boundary. By applying Equation 10 to all elements of z, we defined the probability transition matrix for a single mutation $U(n_x,\lambda)$. The number of mutations n introduced in each offspring was Poisson-distributed with parameter $u = 1$, a value that conforms to estimates of mutation rates in *Drosophila* (HAAG-LIAUTARD *et al.* 2007). Taking account of the variation in the number of mutations per time unit, the mutational probability transition matrix was

$$U(n_x,\lambda) = \sum_{n=0}^{\infty} Pr(n) \times [U(n_x,\lambda)]^n \quad (11).$$

Each cohort contributed to each age-specific *pdf* of phenotypes in proportion to the product of its current fecundity and fractional representation of the population. Given the vertical vector of phenotypic probabilities at time t, $p_{x,y,t}$, the *pdf* of mortality phenotypes of the offspring cohort after mutation specific to some age of expression x was

$$p_{x,1,t+1} = U(n_x,\lambda,u) \cdot \frac{\sum_y^Y \pi_{y,t} \cdot m_y \cdot p_{x,y,t}}{\pi^{'}_{1,t+1}} \quad (12).$$

The phenotypic effects of mutations are expected to be greatest with high n and low λ (POON and OTTO 2000). To explore the consequences of changing these mutational parameters on mutation-selection equilibrium and mutation accumulation, we considered each of $\lambda ?\{50, 100, 150, 200\}$. Complexity is a central component of Fisher's geometric model and some studies have suggested that the complexity of phenotypic traits may change as an organism ages (KAPLAN *et al.* 1991; LIPSITZ and GOLDBERGER 1992 but see GOLDBERGER *et al.* 2002; VAILLANCOURT and NEWELL 2002). We investigated how complexity affected age-related changes in mutational effects by considering a variety of age-specific functions of n. First we considered the scenario in which n is constant across all ages (age-independent complexity), with$n?\{10, 15, 20, 25\}$. In addition, we explored what happens when complexity changes with age (age-dependent complexity). Specifically, we considered what happens if 1) complexity increases between adult age-classes, $n_x = \{10, 10, 20\}$, 2) complexity decreases between adult age-classes, $n_x = \{20, 20, 10\}$, 3) complexity increases between juvenile and adult age-classes, $n_x = \{10, 20, 20\}$, and 4) complexity decreases between juvenile and adult age-classes, $n_x = \{20, 10, 10\}$. Scenarios 1-2 were investigated to see if changes in complexity caused qualitative shifts in the degree to which senescence evolves in reproductive age classes. Scenarios 3-4 were investigated to see how changes in complexity caused equilibrium mortality to diverge between the juvenile and the early adult age classes (recall that selection for both juvenile and early adult survival are equal because juveniles cannot reproduce).

Mutation-selection balance and mutation accumulation: All simulations were allowed to evolve for T generations, defined as the point at which none of the phenotypic distributions deviated from those at generation $T - 1$ to the resolution limit of R 2.5.1. These distributions defined the mutation-selection equilibrium specific to the population with parameters m_x, n_x, λ and u. We then removed selection from the populations by changing the survival function to $P_z = 1$ and allowing the populations to evolve for an additional 50 time units. We attributed the changes in the mean and variance of age-specific mortality between generations $T + 50$ and T to the effects of *de novo* mutation accumulation.

$\pm\infty =\neq\sim \times\div !? <\ll>\gg\leq\geq \mp \cong\approx\equiv \forall\partial\sqrt{\sqrt[3]{\sqrt[4]{a}}}\cup\cap\emptyset\%degdegFdegC\Delta\exists \ni\ni\leftarrow\uparrow\rightarrow\downarrow\leftrightarrow \pm\alpha\beta\gamma\delta\epsilon\varepsilon\theta\vartheta\mu\pi\rho\sigma\tau\phi\omega \cdot \vdots \cdots \ddots$.